

## From correlations to universal behavior in few-nucleon systems

Alejandro Kievsky<sup>1,\*</sup>, Mario Gattobigio<sup>2,\*\*</sup>, Luca Girlanda<sup>3,\*\*\*</sup>, and Michele Viviani<sup>1,\*\*\*\*</sup>

<sup>1</sup>Istituto Nazionale di Fisica Nucleare, Sezione di Pisa, Largo B. Pontecorvo, 56127 Pisa, Italy

<sup>2</sup>Université Côte d'Azur, CNRS, Institut de Physique de Nice, 1361 route des Lucioles, 06560 Valbonne, France

<sup>3</sup>Dipartimento di Matematica e Fisica "E. De Giorgi", Università del Salento, I-73100 Lecce, Italy

**Abstract.** The deuteron, the only two-nucleon bound state, has a shallow character: its binding energy is strictly related to zero-energy parameters, the triplet scattering length  ${}^3a_{np}$  and triplet effective range  ${}^3r_{np}$ . This fact places the deuteron inside the universal window, a region in which systems having a large value of the two-body scattering length are located. When the scattering length is large compared to the interaction range certain types of correlations can be observed. Increasing the number of nucleons these correlations are responsible for the particular spectrum of light nuclei as for example the lack of excited states in three- and four-nucleon systems. In this presentation some constraints imposed by the large values of the singlet and triplet scattering lengths in the spectrum of light nuclear systems are discussed.

### 1 Introduction

When the kinetic and potential energies are such that their difference is almost zero the system is close to support a bound state. The scattering length is large and negative, and a virtual state is located close to the zero-energy threshold. With a small change of the system parameters, the scattering lengths jumps from  $-\infty$  to  $+\infty$  and the virtual state transforms into a bound state. In this particular region, when the scattering length is large with respect to the interaction range, the bound (or virtual) state has a shallow character. It is worth to note that weakly bound systems define a class of universality. Due to the large tail of the wave function, the particles stay most of the time outside the interaction range and many of their properties can be explained in terms of the probability to be in that region. This probability is well estimated by the relation  $1 - r_e/a$ , with  $r_e$  the effective range and  $a$  the scattering length. Close to the unitary limit,  $a \rightarrow \infty$ , the ratio  $r_e/a$  has a small value. Moreover these two quantities determine the  $s$ -wave phase-shift  $\delta$  at low energies through the effective range expansion

$$k \cot \delta = -\frac{1}{a} + \frac{1}{2}r_e k^2 \dots \quad (1)$$

with the energy  $E = \hbar^2 k^2/m$ . From the experimental point of view, these two quantities are extracted from the phases analyzing their behavior at very low energies, when the effective range function,  $S_k = k \cot \delta$ , reaches a linear dependence in terms of the energy. Accepted values in the case of two nucleons are  ${}^3a_{np} = 5.419(7)$  fm

and  ${}^3r_{np} = 1.753(8)$  fm for the spin  $S = 1$  state and  ${}^1a_{np} = -23.740(20)$  fm and  ${}^1r_{np} = 2.77(5)$  fm for the spin  $S = 0$  state, see Ref.[1] and references therein. In the case of two neutrons the quantities in the  $S = 0$  state are  ${}^1a_{nn} = -18.90(40)$  fm and  ${}^1r_{nn} = 2.75(11)$  fm. For two protons the values are  ${}^1a_{pp} = -7.8063$  fm and  ${}^1r_{pp} = 2.773(14)$  fm. However after subtracting the electromagnetic contribution, the scattering length results  ${}^1a_{pp} = -17.137$  fm. Though there is some model dependence in subtracting the electromagnetic contribution, all values of these quantities are such that the two-nucleon system in both spin states is located close to the unitary limit.

A model independent description of the physics inside the unitary window can be given by an effective field theory (EFT) based on the separation of scales between the typical momenta  $Q \sim 1/a$  of the system and the underlying high momentum scale  $\sim 1/\ell$ , with  $\ell$  a typical range of the system [2–5]. This condition is well fulfilled in nuclear physics and this approach is known as pionless-EFT. Using EFT one can systematically improve the prediction of the observables. For instance the effective range expansion can be reproduced by such an expansion. At leading order (LO) the information encoded in the scattering length  $a$  is introduced, whereas the finite-range nature of the interaction, represented by the effective range  $r_e$ , is found at the next-to-the-leading order (NLO). In addition, inside the unitary window, there is an energy pole close to the two-particle threshold. The extension of the effective range function to the negative energy pole results in

$$k_d = \frac{1}{a} + \frac{1}{2}r_e k_d^2 \dots \quad (2)$$

where  $E_2 = -\hbar^2 k_d^2/m$  is the energy of the virtual or bound state.

\*e-mail: kievsky@pi.infn.it

\*\*e-mail: mario.gattobigio@univ-cotedazur.fr

\*\*\*e-mail: girlanda@le.infn.it

\*\*\*\*e-mail: viviani@pi.infn.it

The most remarkable property of systems at the unitary limit appears in the three-body system where the Efimov effect can be observed [6, 7]. When the strength of the two-body interaction is such that there is a bound state at zero-energy, an infinite tower of geometrically distributed energy states appears in the three-body system with the energy threshold  $E_3 = 0$  as an accumulating point. The energy ratio of successive levels  $E_3^{n+1}/E_3^n = e^{-2\pi/s_0}$  is a universal constant, with  $s_0$  depending on the mass ratio of the constituents; for three equal bosons  $s_0 \approx 1.00624$  so that  $e^{-2\pi/s_0} \approx (1/22.7)^2$ . This effect, predicted by V. Efimov around 50 years ago, was observed 35 years after its prediction by the group of R. Grimm [8]. An enormous amount of work, experimental as well as theoretical, has been, and still is, dedicated to study this phenomenon. An introduction to this sector of research can be found in the following reviews [9–16] and references therein.

In the present work we discuss a description of systems inside the unitary window based on a gaussian potential. We call this a gaussian characterization of the window and use the characterization to link different systems along the window and to study the appearance of correlations. As a difference to the standard use of the EFT framework, the gaussian characterization treats at the same level the scattering length and effective range [17–22], so many times the obtained results have to be compared to the NLO of the EFT framework.

## 2 Gaussian characterization of the two-nucleon system

The dynamics of two-body systems inside the universal window is highly independent of the details of their mutual interaction. This is motivated by Eq.(1) and (2): the presence of the shallow state allows for a second order expansion of its energy in  $r_e/a$  introducing a strict correlation between the low energy parameters  $a$ ,  $k_d$  and  $r_e$

$$k_d^{-1} = \frac{a}{2} \left( 1 + \sqrt{1 - 2r_e/a} \right). \quad (3)$$

When this relation is fulfilled with an error at the level of  $(r_e/a)^2$ , the bound or virtual state can be considered shallow. Moreover, these quantities completely determine the  $S$ -matrix of systems having one bound or virtual state

$$\mathcal{S}(k) = \frac{k + ik_d}{k - ik_d} \frac{k + i/r_B}{k - i/r_B}, \quad (4)$$

where we have introduced the length  $r_B = a - 1/k_d$ .

To highlight the universal properties of systems belonging to the unitary window, we propose to study the two-nucleon system using of a two-parameter short-range potential. We consider this potential a minimal low-energy representation of the two-particle interaction fixed by two low-energy data,  $a$  (or  $k_d$ ) and  $r_e$  (or  $r_B$ ). Specifically we use a Gaussian potential

$$V(r) = V_0 e^{-r^2/r_0^2}, \quad (5)$$

where  $r$  is the interparticle distance, while the strength  $V_0$  and the range  $r_0$  are parameters useful to explore the

low-energy dynamics associated with the existence of one (bound or virtual) state close to threshold. In Fig.1 we show how we proceed to characterize the unitary window using the gaussian potential. In the upper panel the solid circles indicate the location of the NN system inside the unitary window. The circles are placed using the corresponding experimental data (in the  $pp$  case electromagnetic effects have been subtracted). The solid line encompasses the solutions of the Schrödinger equation using the gaussian potential with variable strength and range. In fact, the only condition imposed to find the gaussian curve is to limit the gaussian potential to support one bound state for positive values of  $a$  and to have no bound states for negative values of  $a$ . Once these conditions are verified the results of a generic gaussian potential lie on the solid curve. The specific values of the gaussian parameters necessary to describe a particular system are given in the bottom panel from the position of each system on the  $x$ -axis. As a example a gaussian potential with a range  $r_0 = 1.55$  fm is able to describe simultaneously the triplet  $np$  scattering length, the effective range and the deuteron binding energy. In the caso of the  $0^+$  states, the  $np$ ,  $nn$  and  $pp$  systems are well described by a gaussian of range  $r_0 = 1.85$  fm.

Different points along the gaussian curve are related trough the running of the gaussian strength

$$\frac{V_0 m r_0^2}{\hbar^2} = C_0 \left( 1 + \alpha_1 \frac{r_0}{a} + \alpha_2 \left( \frac{r_0}{a} \right)^2 + \dots \right) \quad (6)$$

where  $C_0 = 2.6840$  is the value at which a bound state starts to be supported by the potential and  $\alpha_1, \alpha_2$  are constants, the same for all gaussian potentials [23, 24]. The above equation can be used to connect different systems lying on the gaussian curve. For example the gaussian curve can be designed using a gaussian potential with constant range and variable strength. The complete curve can be explored in this way and the above formula relates the strength of the gaussian potential to the different values of the scattering length. Constructing the curve in this way the values of the ratio  $r_e/a$  at which specific systems are located (those indicated by the symbols in Fig.1) will be reached. Therefore a second possible movement on the curve would be to vary the strength  $V_0$  and the range  $r_0$  maintaining fixed the ratio  $r_e/a$ . The above equation relates the pairs of values  $r_0, V_0$  needed to perform this action. It should be noted that systems having the same ratio  $r_e/a$  are connected by a scale transformation:  $a \rightarrow \lambda a$  and  $k_d \rightarrow k_d/\lambda$  implies  $r_B \rightarrow \lambda r_B$  and  $r_e \rightarrow \lambda r_e$ .

When the interaction between two particles is strongly repulsive at short distances the two-body system is, as a consequence, highly correlated. For bound systems the probability to be inside the repulsive core is very small. Accordingly, the wave function in that region is almost zero and increases rapidly towards the attractive region. Therefore the total energy results from a big cancellation between the kinetic and potential energy. Systems such as the deuteron are examples of this kind of correlation. It is interesting to analyze the description of these systems in terms of the low-energy parameters. Outside the in-

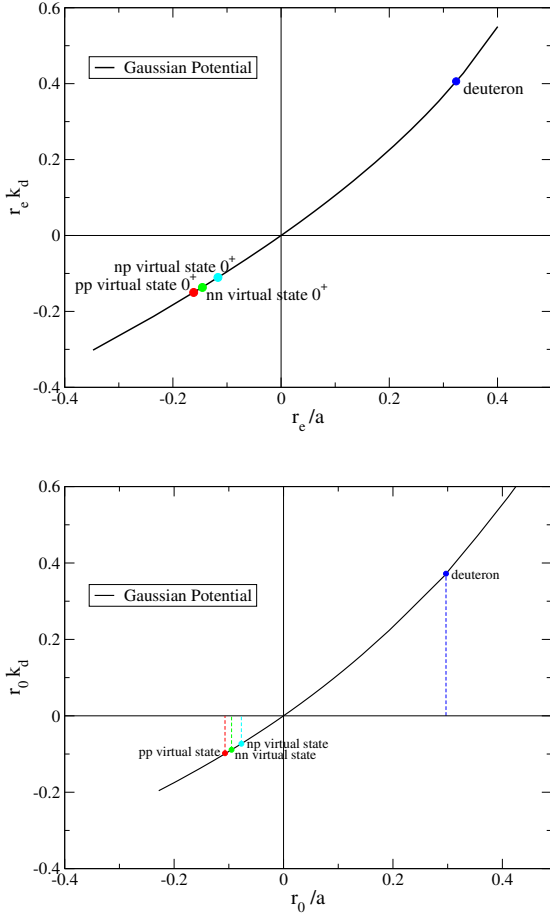


**Figure 1.** Upper panel: the binding momentum as a function of the scattering length (both in units of the effective range) for a gaussian potential. Specific systems are shown by colored symbols. Bottom panel: the binding momentum as a function of the scattering length (both in units of the gaussian range). The position onto the x-axis of the indicated systems is given.

interaction region the  $s$ -wave reduced wave function of the system is

$$\psi_B(r \rightarrow \infty) = C_a e^{-k_d r}, \quad (7)$$

where  $C_a$  is the asymptotic normalization constant well described, inside the unitary window, by the relations

$$C_a^2 = 2k_d \frac{1}{1 - k_d r_e} = 2k_d e^{2k_d r_B}. \quad (8)$$

These relations are fulfilled up to second order in the ratio  $r_e/a$ . At the same order the mean square radius results

$$\langle r^2 \rangle = \frac{a^2}{8} \left[ 1 + \left( \frac{r_B}{a} \right)^2 \right] = \frac{1}{8k_d^2} e^{2k_d r_B}. \quad (9)$$

Both observables are governed by the scaling function  $f_{sc} = e^{2k_d r_B}$ . At the same order, the probability  $P_e$  of the particles to be in the classical forbidden region is defined as

$$P_e = C_a^2 \int_{2r_B}^{\infty} e^{-2k_d r} dr = \frac{C_a^2}{2k_d} e^{-4k_d r_B} = \frac{1 - k_d r_e}{e^{-4k_d r_B}} = e^{-2k_d r_B}, \quad (10)$$

where we have identified  $2r_B = r_e a k_d$  as the lower limit for two particles to be considered outside the interaction region [21]. Very close to the unitary limit  $P_e \approx 1 - r_e/a$ . For weakly bound systems  $P_e$  is governed by the ratio  $2k_d r_B$ , therefore we consider the systems inside the unitary window as strongly correlated. In the Table 1 we give the experimental values for the deuteron observables (second column) and the calculated values using the scaling function  $f_{sc}$  (third column). As can be seen the experimental values are estimated well below a 1% accuracy. Better than the expected error given by  $(r_e/a)^2$  which for the  $S = 1$  state is about 0.1.

$E$ (MeV)	2.224575(9)	2.223
$C_a$ (fm $^{-1/2}$ )	0.8781(44)	0.8786
$\sqrt{\langle r^2 \rangle}$ (fm)	1.97535(85)	1.971
$P_e$		0.601

**Table 1.** Experimental values (second column) and calculated values (third column) of the indicated observables.

### 3 The universal window for $A \leq 6$

The gaussian characterization introduced at the level of two particles can be extended to describe a general number of particles. In this case the potential energy is

$$V = V_0 \sum_{i < j} e^{-r_{ij}^2/r_0^2}, \quad (11)$$

and the unitary window can be explored by varying the parameters of the gaussian potential. Though the above potential applies well for equal boson systems, in the case of nucleons the potential could be different in the different spin-isospin states. Accordingly we extend the above definition to

$$V = V_0 \sum_{i < j} e^{-r_{ij}^2/r_0^2} \mathcal{P}_{01} + V_1 \sum_{i < j} e^{-r_{ij}^2/r_1^2} \mathcal{P}_{10}, \quad (12)$$

where  $\mathcal{P}_{01}$  projects on spin-isospin channels  $S = 0, T = 1$  and  $\mathcal{P}_{10}$  projects on spin-isospin channels  $S = 1, T = 0$ . Due to antisymmetrization these two channels correspond to an  $s$ -wave interaction, therefore the gaussian parameters can be fixed by the low energy  $s$ -wave parameters. In order to maintain low the number of parameters in the following we explore the unitary window using the same range values,  $r_0 = r_1$ , in both spin states. It is interesting to notice that in this case and when the two terms are at the unitary limit, the potential results [23]

$$V = 2.6840 \frac{\hbar^2}{m r_0^2} \sum_{i < j} e^{-r_{ij}^2/r_0^2}, \quad (13)$$

and the binding momentum for  $A = 3, 4$  are [19]

$$K_3 = \frac{0.4883}{r_0}, \quad (14)$$

$$K_4 = \frac{1.1847}{r_0}. \quad (15)$$

To determine the binding energies at the unitary limit of the three- and four-nucleon systems, the range of the gaussian potential has to be known. In order to determine the range, we proceed in the following way. In Fig.2 we show the gaussian characterization of the universal window for three- and four nucleons obtained using a gaussian potential having equal range in both spin channels and the two strengths,  $V_0$  and  $V_1$ , related to follow the nuclear cut, defined as the path in which the singlet and triplet  $np$  scattering lengths have a fixed ratio  $^1a_{np}/^3a_{np} = -4.3$  (see Refs.[19, 25]). In the figure the solid green square and solid red square show the position of  $^3\text{H}$  and  $^4\text{He}$  on the gaussian curve. In fact at those positions the ratio  $\kappa_N/k_d = \sqrt{E_N/E_2}$  correspond to the experimental ratios. For  $N = 3$ ,  $\sqrt{E_3/E_2} = 3.81$ , whereas for  $N = 4$ ,  $\sqrt{E_4/E_2} = 13.13$ . The corresponding values at the x-axis are  $k_d r_0 = 0.457$ , for  $N = 3$ , and  $k_d r_0 = 0.481$ , for  $N = 4$ . From the deuteron binding momentum  $k_d = 0.231 \text{ fm}^{-1}$  we can determine the ranges  $r_0^{(3)}$  and  $r_0^{(4)}$ . With these ranges the following gaussian potentials

$$V = V_0 \sum_{i<j} e^{-(r_{ij}/r_0^{(N)})^2} \mathcal{P}_{01} + V_1 \sum_{i<j} e^{-(r_{ij}/r_0^{(N)})^2} \mathcal{P}_{10} \quad (16)$$

describe simultaneously the experimental values of  $E_N$  and  $E_2$  at the position of the gaussian curve indicated by the green square ( $N = 3$ ) and red square ( $N = 4$ ) in the figure. From the obtained ranges we can determine the binding energies at the unitary limit.

$$E_3 = 0.4883 \frac{\hbar^2}{m[r_0^{(3)}]^2} = 2.54 \text{ MeV}, \quad (17)$$

$$E_4 = 1.1847 \frac{\hbar^2}{m[r_0^{(4)}]^2} = 13.5 \text{ MeV}. \quad (18)$$

The above values are the values at unitary if the systems follow the nuclear cut moving from the physical point to the unitary limit. To check to which extend the gaussian path encodes movements along the unitary window we can scale one of the widely used NN potentials, the Argonne AV14 potential [26]. The AV14 potential can be cast in the following way

$$V(i, j) = \sum_{p=1,14} V_p(r_{ij}) \mathcal{O}_{ij}^p = \sum_{STv} V_v^{ST}(r_{ij}) \mathcal{O}_v^{ST}(ij) \quad (19)$$

with  $\mathcal{O}_{ij}^p$  the 14 operators that characterize the potential. In the last equality the potential is given in the four spin-isospin channels  $ST = 01, 10, 00, 11$ . To bring the potential to the unitary limit the spin-isospin channels  $ST = 01, 10$  are scaled by 1.0633 and 0.8 respectively. With this calibration the two scattering lengths,  $^1a_{np}$  and  $^3a_{np}$ , are close to infinity. The binding energy of  $^3\text{H}$  calculated with the scaled potential results  $B(^3\text{H}) = 2.4 \text{ MeV}$ , very close to the value predicted by the gaussian characterization. This numerical observation confirms the low sensitivity to the interaction details this particular region has.

Figure 2 shows another interesting question regarding the existence of excited states in  $^3\text{H}$  and  $^4\text{He}$ . At unitarity the spectrum of  $^3\text{H}$  has the Efimov structure, an infinite tower of geometrically distributed states accumulating at  $E = 0$ . In the figure the first state is shown with

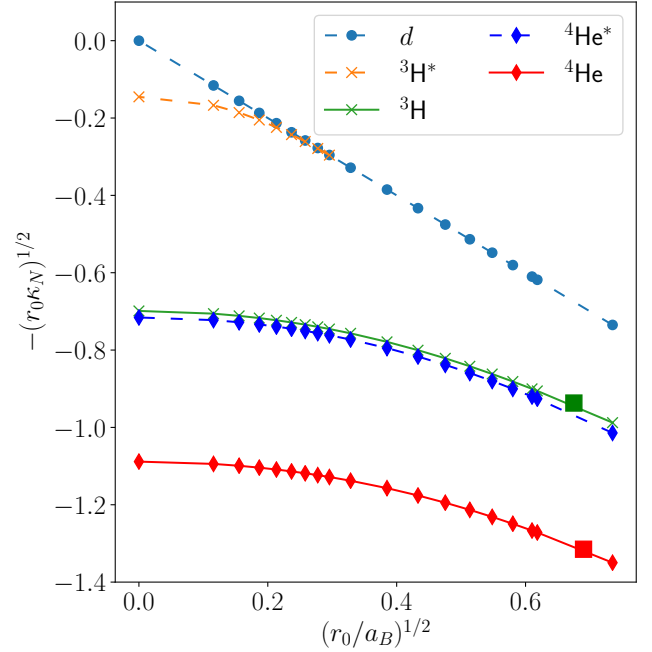


**Figure 2.** The binding momentum for  $N = 2, 3, 4$  as a function of the two-body binding momentum  $k_d = 1/a_B$ , both in units of the gaussian range, calculated using the spin-dependent gaussian potential.  $^3\text{H}^*$  and  $^4\text{He}^*$  are the first excited state for the three- and four-nucleon system, respectively.

the orange dashed line. As the parameters of the gaussian potential are varied to follow the nuclear cut, the excited state disappears very soon crossing the two-body threshold and becoming a virtual state [20]. The excited state disappears around a value of the triplet scattering length of 18 fm, very far from the physical point. Therefore we can conclude that the absence of excited states in the three-nucleon system is related to the position of the deuteron in the universal window and can be explained using the gaussian characterization of the window. In the case of  $^4\text{He}$ , Fig.2 shows that there is an excited state at unitarity and that the excited state remains along the path (blue diamonds). However in the figure the Coulomb interaction has not been considered. When it is taken into account, the three-nucleon systems,  $^3\text{H}$  and  $^3\text{He}$ , split and at the same time the excited state of  $^4\text{He}$  move into the continuum [19].

We now comment on the formation of the  $A = 6$  nuclei as emerging from the unitary limit. This is illustrated in Fig.3. At unitarity, the potential of Eq.(13) is used to solve the Schrödinger equation for  $A \geq 3$ . Due to antisymmetrization of the wave function, the  $A = 6$  nuclei result unbound below the  $^4\text{He}$  threshold. Differently from what happens at the physical point, at unitarity the  $np$  system has zero energy and, therefore  $^6\text{He}$  and  $^6\text{Li}$  have the same threshold represented by the  $^4\text{He}$  binding energy. As the strength of the potential increases along the nuclear cut the two nuclei appear, first  $^6\text{Li}$  (violet squares) and then  $^6\text{He}$  (red stars). The exact position of these nuclei on top of the gaussian characterization is discussed in Ref.[19]. In the figure the energies are given in units of the triton energy

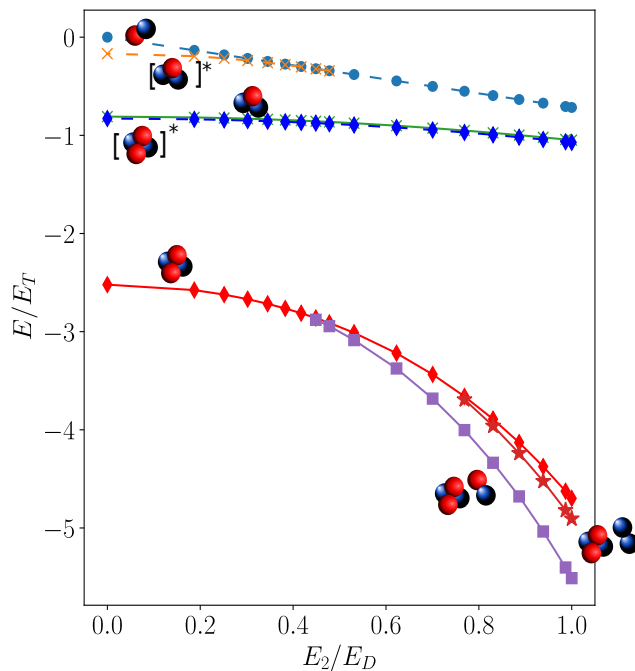


**Figure 3.** The energies of the two-, three-, four- and six-nucleon systems, in units of the triton binding energy  $E_T$ , as a function of the two-body energy, in units of the deuteron energy. Symbols indicate the different nuclei (red and blue circles representing protons and neutrons respectively). The '\*' indicates excited states.

$E_T$  as a function of the two-body energy in units of the deuteron energy.

## 4 Conclusions

In the present work we have discussed the gaussian characterization of the unitary window in the case of few-nucleon systems. Systems belonging to this window show low sensitivity to the interaction details. The dynamics is governed by the scattering length and by the location on the unitary window given by the ratio  $r_e/a$ . The gaussian paths are useful to connect different systems, for example atomic and nuclear systems, or the same system in different spin channels, as the NN system in  $S = 0$  or  $S = 1$ . They are also useful to follow real (or ideal) movements of the systems inside the window. Though in nuclear systems at present it is not possible to perform experiments in which the nuclear interaction is changed, this can be achieved for atomic systems in traps using Feshbach resonances. For these particular systems, trapped cold atoms, it was shown that a particular class of universal properties appears known as van der Waals universality. In Ref. [21] this property has been discussed showing that this class of universality is well described by the gaussian characterization. This is a manifestation of two facts; from one side, due to the low importance on the details of the interaction, the real interaction between two-particles can be effectively represented by a two-parameter potential as a

gaussian. At that point, movements of the systems inside the unitary window can be followed by varying the parameters of that effective potential. On the other hand, movements along the window can be followed by scaling the original potential with the result that the scaled potential follows closely the gaussian path. In the present discussion we have shown explicitly this fact by constructing a two-body gaussian potential able to describe simultaneously the triton and deuteron binding energies and, with a different range, the alpha particle and the deuteron. Then, using the range of those gaussian potentials, we have predicted the corresponding binding energies at unitarity. To verify the quality of this procedure we have proposed an ideal experiment by scaling the spin-isospin channels  $S, T = 0, 1$  and  $1, 0$  of the AV14 potential in order to bring the system at the unitary limit. Then we have calculated the  $^3\text{H}$  binding energy at unitarity, using the scaled potential, and surprisingly the energy value resulted very close to that one predicted by the gaussian potential showing that the scaled potential follows the gaussian path.

One important property of the gaussian characterization is the possibility of connecting the physical points to the unitary limit allowing the study of the nuclear levels at this limit. In this respect the unitary limit can be seen as a mirror of the nuclear levels in which the scale symmetry is better realized. First of all we have shown the evolution of the excited states. At unitarity the three-nucleon system described by the potential of Eq.(13) has an infinite number of excited states geometrically distributed (Efimov spectrum). By varying the strength of the interaction following the nuclear cut, the system moves away from that limit and the excited states disappear one by one, the last one when the  $np$  scattering length is around 18 fm. In the case of  $^4\text{He}$ , the excited state is present along the gaussian path and its evolution onto a resonance state depends on the inclusion of the Coulomb interaction. Interestingly we have shown that  $^6\text{He}$  and  $^6\text{Li}$  are not bound at the unitary limit, their binding strongly depends on the deuteron one. They emerge as stable states close to the point at which the excited state of the triton disappears. We can conclude that the particular spectrum of the light nuclei is strongly determined by the position of the deuteron and the  $0^+$  virtual states inside the unitary window. With the corresponding scattering lengths and effective ranges as the only input parameters, the  $A \leq 6$  spectrum can be predicted and continuously linked to the unitary point. The extension of the present analysis up to  $^{12}\text{C}$  is at present underway.

## References

- [1] M. Piarulli, L. Girlanda, R. Schiavilla, R. Navarro Pérez, J.E. Amaro, and E. Ruiz Arriola, *Phys. Rev. C* **91**, 024003 (2015)
- [2] H.W. Hammer, S. König S, and U. van Kolck, *Rev. Mod. Phys.* 92:025004 (2020)
- [3] U. van Kolck, *Nucl. Phys. A* 645:273 (1999)
- [4] P. Bedaque, H.W. Hammer, and U. van Kolck, *Phys. Rev. Lett.* 82:463 (1999)

- [5] P. Bedaque, H.W. Hammer, and U. van Kolck, *Nucl. Phys. A* **646**:444 (1999)
- [6] V. Efimov, *Phys. Lett. B* **33**:563 (1970)
- [7] V. Efimov, *Sov. J. Nucl. Phys.* **12**:589 (1971)
- [8] T. Kraemer, et al., *Nature* **440**:315 (2006)
- [9] E. Braaten, and H.W. Hammer, *Phys. Rep.* **428**:259 (2006)
- [10] H.W. Hammer, and L. Platter, *Eur. Phys. J. A* **32**:113 (2007)
- [11] L. Platter, *Few-Body Syst.* **46**:139 (2009)
- [12] F. Ferlaino, and R. Grimm, *Physics* **3**:9 (2010)
- [13] F. Ferlaino, et al., *Few-Body Syst.* **51**:113 (2011)
- [14] T. Frederico, et al., *Few-Body Syst.* **51**:87 (2011)
- [15] C.H. Greene, P. Giannakeas, J. Pérez-Ríos, *Rev. Mod. Phys.* **89**:035006 (2017)
- [16] P. Naidon, S. Endo, *Rep. Prog. Phys.* **80**:056001 (2017)
- [17] A. Kievsky, A. Polls, B. Juliá Díaz, and N.K. Timofeyuk, *Phys. Rev A* **96**, 040501(R) (2017)
- [18] A. Kievsky, A. Polls, B. Juliá Díaz, N.K. Timofeyuk, and M. Gattobigio, *Phys. Rev A* **102**, 063320 (2020)
- [19] M. Gattobigio, A. Kievsky, and M. Viviani, *Phys. Rev. C* **100**, 034004 (2019).
- [20] A. Deltuva, M. Gattobigio, A. Kievsky, and M. Viviani, *Phys. Rev. C* **102**, 064001 (2020).
- [21] A. Kievsky, M. Gattobigio, L. Girlanda, and M. Viviani, *Annu.Rev.Nucl.Part.Sci.* **2021.71**:465-90
- [22] P. Recchia, A. Kievsky, L. Girlanda, and M. Gattobigio, *Phys. Rev. A* **106**, 022812 (2022)
- [23] R. Álvarez-Rodríguez, A. Deltuva, M. Gattobigio, A. Kievsky, *Phys. Rev. A* **93**, 062701 (2016)
- [24] Bazak B, Eliyahu M, van Kolck U. *Phys. Rev. A* **94**, 052502 (2016)
- [25] A. Kievsky, M. Gattobigio, *Few-Body Syst.* **57**:217 (2016)
- [26] R.B. Wiringa, R.A. Smith, and T.L. Ainsworth, *Phys. Rev. C* **29**, 1207 (1984)